Progress In Electromagnetics Research Letters, Vol. 85, 31–36, 2019

Performance Analysis of Refined Induction Motor Models Considering Iron Loss

Wan Jun Yin[1, 2] and Tao Wen[1, *]

Abstract—In the applications such as induction motor efficiency optimization and electric vehicle speed control, the influence of the iron loss cannot be ignored. In order to improve the running efficiency of induction motor, the ordinary differential equations (ODE) and difference equations (DE) of induction motors considering iron loss have been established. The results show that the proposed refined ordinary differential equations and difference equations of induction motors considering iron loss and its simulation models are believable, and simulated and experiment results have demonstrated that the models perform well.

1. INTRODUCTION

Among various types of AC motors, induction motors, especially squirrel cage motors, are most commonly used in industry due to their economy, reliability, and durability. However, the research on the establishment and control of motor model is often considered ideal, without considering the iron loss. In practice, iron loss resistance is a function of frequency, and the equivalent magnetization reactance is also a variable value and a function of main magnetic flux [1, 2]. In order to control it accurately, it is necessary to study the simulation of motor control considering the actual situation. Although the development of variable frequency speed regulation technology has greatly reduced the losses of induction motors, the problem of low light load operation efficiency still exists. Today, energy problem is becoming more and more serious. It is of great significance to study the energy saving problem of variable frequency speed regulating induction motor under light load and improve its operation efficiency for saving energy and controlling environmental pollution. The mathematical models of ordinary differential equation and difference equation of induction motor considering the effect of equivalent resistance of iron loss are established.

Because the states and parameters are separated clearly in the ODE representation of the induction motor mathematical model, establishing a parameter variable simulation model is very easy [3–7], and the parameter can be changed during the simulation in arbitrary form.

2. ODE AND DE OF INDUCTION MOTORS CONSIDERING IRON LOSS

2.1. ODE of Induction Motors Considering Iron Loss

The equivalent Circuit of Induction Motor Considering Iron Loss under dq Axis of Synchronous Rotating Coordinate System is shown in Fig. 1.

Received 16 November 2019, Accepted 5 June 2019, Scheduled 17 June 2019
* Corresponding author: Tao Wen (6600296@sohu.com).
[1]?, School of Mechano-Electronic Engineering, Xidian University, Xi'an 710071, P. R. China. [2] Sichuan Vocational College of Information Technology, Sichuan, Guangyuan 628040, P. R. China.

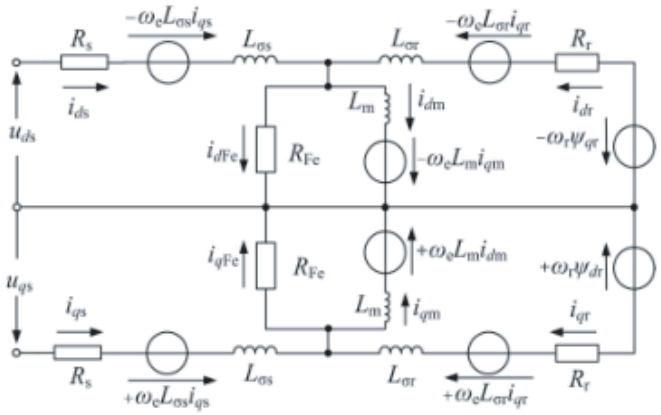

Figure 1. Equivalent circuit of induction motor considering iron loss [1].

Based on Fig. 1 according to the Kirchhoff's law, the voltage equations and current equations of the iron loss equivalent branch are as follows.

$$\begin{cases} L_m \dfrac{di_{dm}}{dt} - \omega_e L_m i_{qm} = i_{dFe} R_{Fe} \\ L_m \dfrac{di_{qm}}{dt} + \omega_e L_m i_{dm} = i_{qFe} R_{Fe} \\ i_{ds} + i_{dr} = i_{dm} + i_{dFe} \\ i_{qs} + i_{qr} = i_{qm} + i_{qFe} \end{cases} \tag{1}$$

the stator side and rotor side voltage equations are given as follows.

$$\begin{cases} R_s i_{ds} - \omega_e L_{\sigma s} i_{qs} + L_{\sigma s} \dfrac{di_{ds}}{dt} + i_{dFe} R_{Fe} = u_{ds} \\ R_s i_{qs} - \omega_e L_{\sigma s} i_{qs} + L_{\sigma s} \dfrac{di_{qs}}{dt} + i_{qFe} R_{Fe} = u_{qs} \\ R_r i_{dr} - \omega_e L_{\sigma r} i_{qr} + L_{\sigma r} \dfrac{di_{dr}}{dt} + L_m \dfrac{di_{dm}}{dt} - \omega_e L_m i_{qm} + \omega_r \psi_{dr} = 0 \\ R_r i_{qr} - \omega_e L_{\sigma r} i_{qr} + L_{\sigma r} \dfrac{di_{qr}}{dt} + L_m \dfrac{di_{qm}}{dt} + \omega_e L_m i_{dm} + \omega_r \psi_{dr} = 0 \end{cases} \tag{2}$$

where i_{ds} and i_{qs} are the d-axis and q-axis stator currents; R_{Fe} is the equivalent iron loss resistance; ω_e is the power angle frequency; ω_r is the rotor electrical angular frequency; i_{dm} and i_{qm} are the d-axis and q-axis magnetizing currents, A; u_{ds} and u_{qs} are the d-axis and q-axis stator voltages; ψ_{dr} and ψ_{qr} are the d-axis and q-axis rotor flux linkages; $L_{\sigma s}$ is the stator leakage inductance; $L_{\sigma r}$ is the rotor leakage inductances; L_m is the mutual inductance; R_s is the stator resistance; R_r is the rotor resistance.

ODE of the induction motor considering the iron loss is as follows.

$$\begin{cases} -\dfrac{(R_s + R_{Fe}) i_{ds}}{L_{\sigma s}} + \omega_e i_{qs} + \dfrac{L_r R_{Fe} i_{dm}}{L_{\sigma s} L_{\sigma r}} - \dfrac{R_{Fe} \psi_{dr}}{L_{\sigma s} L_{\sigma r}} + \dfrac{u_{ds}}{L_{\sigma s}} = \dfrac{di_{ds}}{dt} \\ -\omega_e i_{ds} - \dfrac{(R_s + R_{Fe}) i_{qs}}{L_{\sigma s}} + \dfrac{L_r R_{Fe} i_{qm}}{L_{\sigma s} L_{\sigma r}} - \dfrac{R_{Fe} \psi_{dr}}{L_{\sigma s} L_{\sigma r}} + \dfrac{u_{qs}}{L_{\sigma s}} = \dfrac{di_{qs}}{dt} \\ \dfrac{R_{Fe} i_{ds}}{L_{\sigma s}} + \omega_e i_{qm} - \dfrac{L_r R_{Fe} i_{dm}}{L_m L_{\sigma r}} + \dfrac{R_{Fe} \psi_{dr}}{L_m L_{\sigma r}} = \dfrac{di_{dm}}{dt} \\ \dfrac{R_{Fe} i_{qs}}{L_{\sigma s}} - \omega_e i_{dm} - \dfrac{L_r R_{Fe} i_{qm}}{L_m L_{\sigma r}} + \dfrac{R_{Fe} \psi_{qr}}{L_m L_{\sigma r}} = \dfrac{di_{qm}}{dt} \\ \dfrac{L_m R_r i_{dm}}{L_{\sigma r}} - \left(\dfrac{L_m R_r}{L_r L_{\sigma r}} + \dfrac{R_r}{L_r} \right) \psi_{dr} + (\omega_e - \omega_r) \psi_{qr} = \dfrac{d\psi_{dr}}{dt} \\ \dfrac{L_m R_r i_{qm}}{L_{\sigma r}} - \left(\dfrac{L_m R_r}{L_r L_{\sigma r}} + \dfrac{R_r}{L_r} \right) \psi_{qr} + (\omega_e - \omega_r) \psi_{dr} = \dfrac{d\psi_{qr}}{dt} \end{cases} \tag{3}$$

$$Te = \frac{PL_m}{L_{\sigma r}}\left(i_{qm}\psi_{dr} - i_{dm}\psi_{qr}\right) \tag{4}$$

$$\frac{d\omega_r}{dt} = \frac{P}{J}\left(T_e - T_L\right) \tag{5}$$

where L_s is the stator inductance, L_r the rotor inductances, T_L the load torque, P the number of pole pairs, and J the inertia moment.

2.2. DE of Induction Motors Considering Iron Loss

Similarly, the difference equations can be obtained from ordinary differential equations

$$\begin{cases} i_{ds}(k+1) = \left(1 - \dfrac{(R_s - R_{Fe})T}{L_{\sigma s}}\right) i_{ds}(k) + T\omega_e(k) i_{qs}(k) + \dfrac{Tu_{ds}(k)}{L_{\sigma s}} + \dfrac{L_r R_{Fe} T i_{dm}(k)}{L_{\sigma s} L_{\sigma r}} - \dfrac{R_{Fe} T}{L_{\sigma s} L_{\sigma r}}\psi_{dr} \\ i_{qs}(k+1) = \left(1 - \dfrac{(R_s - R_{Fe})T}{L_{\sigma s}}\right) i_{qs}(k) - T\omega_e(k) i_{ds}(k) + \dfrac{Tu_{qs}(k)}{L_{\sigma s}} + \dfrac{L_r R_{Fe} T i_{qm}(k)}{L_{\sigma s} L_{\sigma r}} - \dfrac{R_{Fe} T}{L_{\sigma s} L_{\sigma r}}\psi_{qr} \\ i_{dm}(k+1) = \left(1 - \dfrac{L_r R_{Fe} T}{L_m L_{\sigma s}}\right) i_{dm}(k) + T\omega_e(k) i_{qm}(k) + \dfrac{R_{Fe} T i_{ds}(k)}{L_m} - \dfrac{R_{Fe} T}{L_m L_{\sigma r}}\psi_{dr}(k) \\ i_{qm}(k+1) = \left(1 - \dfrac{L_r R_{Fe} T}{L_m L_{\sigma r}}\right) i_{qm}(k) - T\omega_e(k) i_{dm}(k) + \dfrac{R_{Fe} T i_{qs}(k)}{L_m} - \dfrac{R_{Fe} T}{L_m L_{\sigma r}}\psi_{qr}(k) \\ \psi_{dr}(k+1) = \left[1 - T\left(\dfrac{L_m R_r}{L_r L_{\sigma r}} + \dfrac{R_r}{L_r}\right)\right]\psi_{dr}(k) + \dfrac{L_m R_r T i_{dm}(k)}{L_{\sigma r}} + T(\omega_e(k) - \omega_r(k))\psi_{qr}(k) \\ \psi_{qr}(k+1) = \left[1 - T\left(\dfrac{L_m R_r}{L_r L_{\sigma r}} + \dfrac{R_r}{L_r}\right)\right]\psi_{qr}(k) + \dfrac{L_m R_r T i_{qm}(k)}{L_{\sigma r}} - T(\omega_e(k) - \omega_r(k))\psi_{qr}(k) \end{cases} \tag{6}$$

where T is the sampling period. The torque equation and motion equation are as follows

$$Te(k) = \frac{PL_m}{L_{\sigma r}}(i_{qm}(k)\psi_{dr}(k) - i_{dm}(k)\psi_{qr}(k)) \tag{7}$$

$$\omega_r(k+1) = (Te(k) - T_L(k))\frac{PT}{J} + \omega_r(k) \tag{8}$$

3. BUILDING SIMULATION MODEL IN MATLAB

Matlab is very popular simulation softwares in the power electronics fields [4–11]. In order to verify the correctness of the induction motor model considering iron loss, a simulation model as shown in Fig. 2 is established.

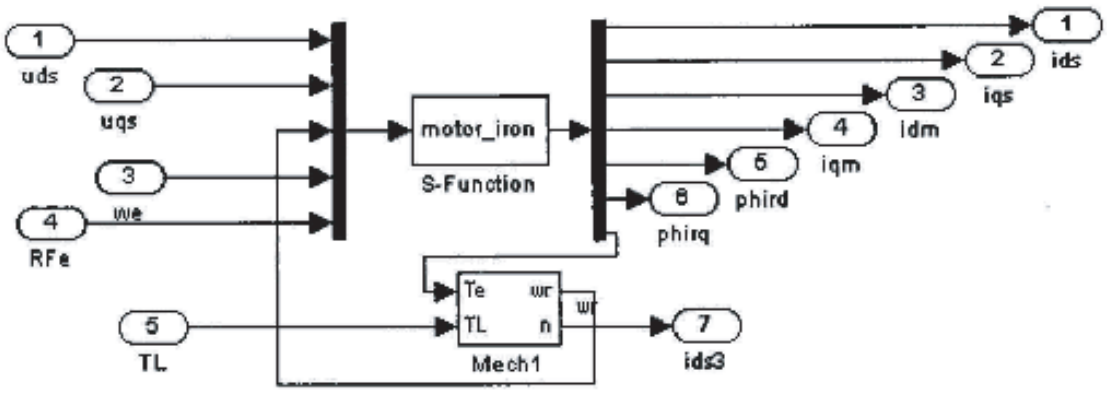

Figure 2. Simulation model of induction motor considering iron loss.

The simulation key C code is as follows:

```
A11=-(Rs+RFe)/LIs;
A13=(Lr*RFe)/(LIs*LIr);
A15=-RFe/(LIs*LIr);
A33=-(Lr*RFe)/(Lm*LIr);
A35=RFe/(Lm*LIr);
A53=(Lm*Rr)/LIr;
A55=-((Lm*Rr)/(Lr*LIr)+(Rr/Lr));
x1=ids+(A11*ids+We*iqs+A13*idm+A15*Psidr+Ud/LIs)*delt;
x2=iqs+(A11*iqs-We*ids+A13*iqm+A15*Psiqr+Uq/LIs)*delt;
x3=idm+((RFe/Lm)*ids+A33*idm+We*iqm+A35*Psidr)*delt;
x4=iqm+((RFe/Lm)*iqs+A33*iqm-We*idm+A35*Psiqr)*delt;
x5=Psidr+(A53*idm+A55*Psidr+(We-Wr)*Psiqr)*delt;
x6=Psiqr+(A53*iqm+A55*Psiqr+(-(We-Wr))*Psidr)*delt;
ids=x1,iqs=x2,idm=x3,iqm=x4,Psidr=x5,Psiqr=x6;
Te=((pm*Lm)/LIR)*(iqm*psidr-idm*psiqr);
Wr=Wr+(((Te-TL)*pm)/J)*delt
n=30*Wr/(pm*3.1415926);
```

4. MODEL VALIDATION

In order to verify the correctness of the proposed user-defined simulation models established, the models are compared with the library model provided by Matlab, and a induction motor is employed in the experiments. The parameters are given in Table 1.

Table 1. Induction motor parameters comparison.

Parameter	Value
Rated power P_N	1.5 kW
Rated voltage U_N	380 V
Rated current I_N	2.75 A
Rated frequency f_N	50 Hz
Rated speed n_N	2800 r/min
Rated Load torque T_N	15.48 Nm
Stator resistance R_s	4.26 Ω
Rotor resistance R_r	4.08 Ω
Stator inductance L_s	0.356 H
Rotor inductance L_r	0.381 H
Mutual inductance L_m	0.338 H
nertia moment J	0.018
Pole pairs p	1
Referred iron loss resistance R_{Fe}	1585

Figure 3 gives the comparison results between the actual operation data and the proposed model simulation curves. The actual induction motor is driven by an inverter employing the variable voltage variable frequency (VVVF) operation mode. The frequency command rises from 0 Hz to 50 Hz within 2 s, and the induction motor runs at no load. It can be seen that the proposed models can give nearly fair numerical analog for the actual induction motor. The correctness and validity of the model are further verified.

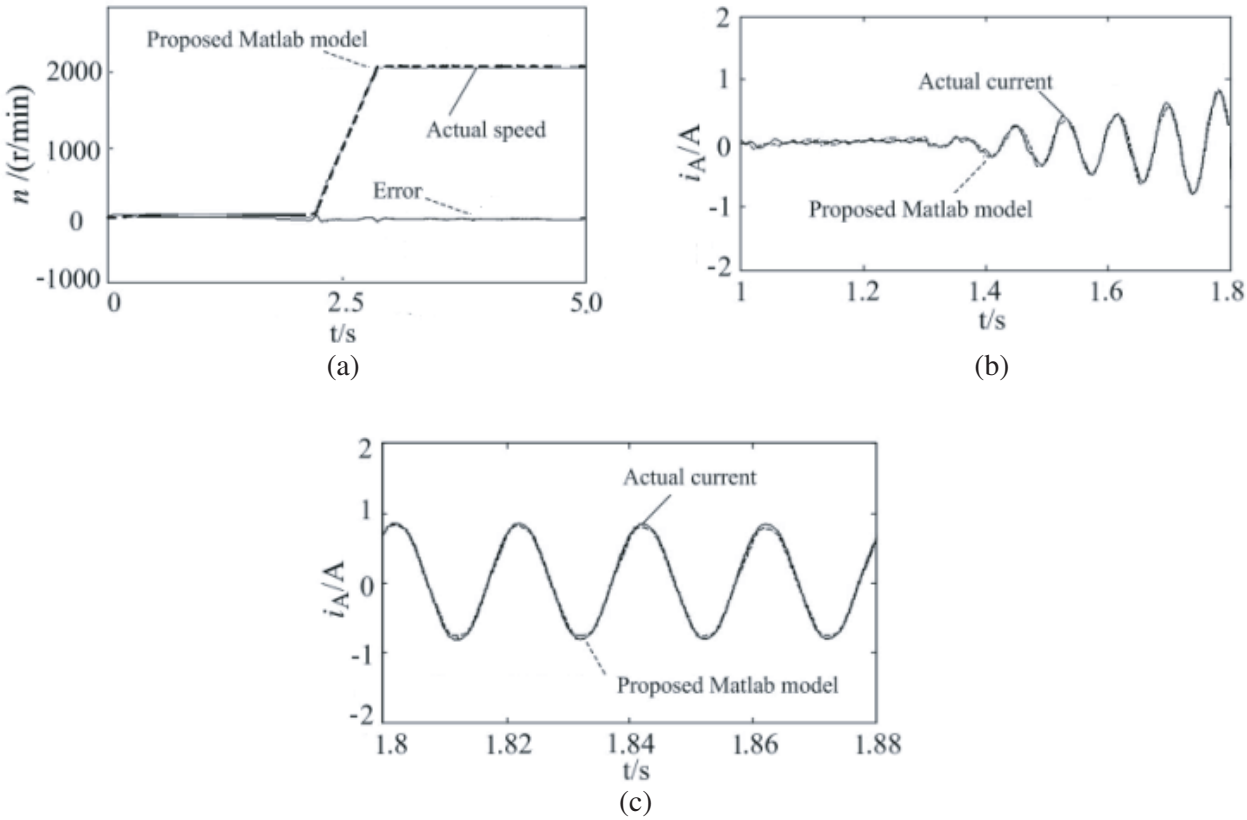

Figure 3. Comparison between numerical solution of proposed simulation model and actual operation data of induction motor. (a) Speed wave forms. (b) Current wave forms comparison when induction motor starts. (c) Current wave forms comparison at steady state.

5. CONCLUSION

In this paper, the ordinary differential equation and difference equation models of induction motor considering iron loss are established and compared with MATLAB motor simulation model. The simulation results verify the accuracy of the model.

In future work, we will explore a simpler and more accurate induction motor model for the purpose of improving the operation efficiency of the motor.

ACKNOWLEDGMENT

This work is partially supported by the Key Program of Guangyuan Municipal Science and Technology Project (2018ZCZDYF016). The authors would like to express their sincere thanks to the referees for their valuable suggestions and comments.

REFERENCES

1. Li, J., F. F. Xiao, and S. Q. Zhang, "Simplified loss model control efficiency optimization algorithm for vector control induction motor drives," *IECON 2017 — 43rd Annual Conference of the IEEE Industrial Electronics Society*, 5178–5183, Beijing, 2017.
2. Li, J., W. Wang, and Y. R. Zhong, "Joint simulation method of PSIM+Matlab for power electronic systems," *Power Electronics*, Vol. 44, No. 5, 86–88, May 2010 (in Chinese).

3. Li, Z., Y. Jiang, and Q. Guo, "Multi-dimensional variational mode decomposition for bearing-crack detection in wind turbines with large driving-speed variations," *Renewable Energy*, Vol. 116, Part B, 55–73, 2016, DOI: 10.1016/j.renene.2016.12.013.
4. Glowacz, A., "Acoustic based fault diagnosis of three-phase induction motor," *Applied Acoustics*, Vol. 137, 82–89, 2018, DOI:10.1016/j.apacoust.2018.03.010.
5. Werner, U., "Vibration control of large induction motors using actuators between motor feet and steel frame," *Mechanical Systems and Signal Processing*, Vol. 112, 319–342, 2018, DOI: 10.1016/j.ymssp.2018.04.033.
6. Caesarendra, W. A., "Review of feature extraction methods in vibration-based condition monitoring and its application for degradation trend estimation of low-speed slew bearing," *Machines*, Vol. 5, No. 4, 2017, DOI:10.3390/machines5040021.
7. Glowacz, A., "Acoustic-based fault diagnosis of commutator," *Motor Electronics*, Vol. 7, No. 11, 2018, DOI: 10.3390/electronics7110299.
8. Singh, G., "Detection of half broken rotor bar fault in VFD driven induction motor drive using motor square," *Mechanical Systems and Signal Processing*, Vol. 110, 333–348, 2018, DOI: 10.1016/j.yrrissp.2018.03.001.
9. Pang, B., G. Tang, and T. Tian, "Rolling bearing fault diagnosis based on an improved HTT transform," *Sensors*, Vol. 18, No. 4, 2018, DOI: 10.3390/s18041203.
10. Glowacz, A. and W. Glowacz, "Vibration-based fault diagnosis of commutator," *Motor Shock and Vibration*, Vol. 2018, Article ID 7460419, 10 pages, 2018, DOI: 10.1155/2018/7460419.
11. Fernandes, J. D., "Wireless monitoring of induction machine rotor physical variables," *Sensors*, Vol. 17, No. 11, 2017, DOI: 10.3390/s17112660.